



This is a repository copy of *Centralized semi-active control of post-tensioned steel frames*.

White Rose Research Online URL for this paper:  
<http://eprints.whiterose.ac.uk/87716/>

Version: Accepted Version

---

**Article:**

Eljajeh, Y. and Petkovski, M. (2015) Centralized semi-active control of post-tensioned steel frames. *Earthquake Engineering & Structural Dynamics*, 44. 79 - 100. ISSN 1096-9845

<https://doi.org/10.1002/eqe.2460>

---

**Reuse**

Unless indicated otherwise, fulltext items are protected by copyright with all rights reserved. The copyright exception in section 29 of the Copyright, Designs and Patents Act 1988 allows the making of a single copy solely for the purpose of non-commercial research or private study within the limits of fair dealing. The publisher or other rights-holder may allow further reproduction and re-use of this version - refer to the White Rose Research Online record for this item. Where records identify the publisher as the copyright holder, users can verify any specific terms of use on the publisher's website.

**Takedown**

If you consider content in White Rose Research Online to be in breach of UK law, please notify us by emailing [eprints@whiterose.ac.uk](mailto:eprints@whiterose.ac.uk) including the URL of the record and the reason for the withdrawal request.



[eprints@whiterose.ac.uk](mailto:eprints@whiterose.ac.uk)  
<https://eprints.whiterose.ac.uk/>

## Centralized semi-active control of post-tensioned steel frames

Yasser Eljajeh<sup>1\*</sup>, Mihail Petkovski<sup>1</sup>

<sup>1</sup>*University of Sheffield, Department of Civil and Structural Engineering, Sir Frederick Mappin Building, Sheffield, UK, S1 3JD.*

### SUMMARY

Centralized semi-active control is a technique for controlling the whole structure using one main computer. Centralized control systems introduce better control for relatively short to medium high structures where the response of any story cannot be separated from the adjacent ones. In this paper, two centralized control approaches are proposed for controlling the seismic response of post-tensioned steel frames. The first approach, the stiffness control approach, aims to alter the stiffness of the PT frame so that it avoids large dynamic amplifications due to earthquake excitations. The second approach, deformation regulation control approach, aims at redistributing the demand/strength ratio in order to provide a more uniform distribution of deformations over the height of the structure. The two control approaches were assessed through simulations of the earthquake response of semi-actively and passively controlled six-story post-tensioned steel frames. The results showed that the stiffness control approach is efficient in reducing the frame deformations and internal forces. The deformation regulation control approach was found to be efficient in reducing the frame displacements and generating a more uniform distribution of the inter-story drifts. These results indicate that centralized semi-active control can be used to improve the seismic performance of post-tensioned steel frames. Copyright © 0000 John Wiley & Sons, Ltd.

Received ...

KEY WORDS: Post-tensioned connections, semi-active control, stiffness control, self-centering.

### 1. INTRODUCTION

#### 1.1. Background

Post-tensioned steel frames were proposed as a replacement of conventional moment resisting frames [1, 2] in seismic applications. The up-to-date research demonstrates that post-tensioning is a good solution for reducing residual drifts and preventing damage in the beams when compared with other passive control systems [3]. Residual deformations can be completely eliminated by following a specific procedure for design of PT frames [4]. Energy dissipation in the connections was provided by yielding top and seat angles [1], yielding bars [2], and friction devices [5]. However, regardless of the type of energy dissipater, PT connections exhibit flag-shaped hysteresis with lower energy dissipation than that in post-Northridge pre-qualified beam-column moment resisting connections [6, 7]. This means that PT frames can be used to eliminate residual deformations but not to reduce the maximum inter-story drifts of equivalent moment resisting frames [8].

Semi-active control of frame structures is an approach that has been progressively developed since the introduction of a semi-active tuned mass damper [9]. Different approaches have been proposed in the literature, including (a) added semi-active dampers [10, 11, 12, 13] (b) stiffness control to

---

\*Correspondence to: University of Sheffield, Department of Civil and Structural Engineering, Sir Frederick Mappin Building, Sheffield, UK, S1 3JD. E-mail: yasser-eljajeh@yahoo.com

avoid resonance of the response [14, 15] and (c) energy dissipation approach to increase energy dissipation capacity of the frame [16, 17]. These approaches can be centralized or decentralized [18]. Centralized systems use one computer to control the whole structure, whereas in decentralized systems the control actions are calculated independently at several control points.

The stiffness control is a centralized approach that has been proposed in previous research work and investigated for braced frames and truss structures. The main part of any algorithm based on the stiffness control approach is the stiffness selection algorithm. The work done by Kobori et al. [14] was the first to use the stiffness control approach to suppress the dynamic response of a three-story steel braced frame. In that work, some evaluative indices were used to assess the response of each possible stiffness pattern. These indices employed coefficients which were not deterministic as their values were based on simulations of the structural response under several earthquakes with different characteristics.

Nemir et al. [15] used the modal energy transference theory to select the optimum stiffness pattern. The selection of the stiffness pattern in their work was based on minimizing the modal energy of the structure. This control however was suitable only for linear systems as their algorithm relied on the modal decomposition of the equation of motion to find the modal energy of the structure at any time. Iskhakov and Ribakov [19] proposed a passive system in which the stiffness of the building is self-adapting by developing damage in the diagonals, and an upgraded optimal semi-active control system, where semi-actively controlled friction connections are used to prevent premature failure of the compressed diagonals. Duerr et al. [20] used a smart spring with a bang-bang algorithm to provide energy dissipation and stiffness control to a four-story structure, which remains elastic during the response.

It should be noted that none of the work on semi-active control using stiffness control approach was done on post-tensioned steel frames. The semi-active techniques for controlling the seismic response of PT frames were first incorporated by Eljajeh and Petkovski [21]. This research was based on a decentralized control approach where the goal was to increase the energy dissipation capacity of each PT connection. The results of the simulations showed reduced SRSS displacements of the frame and improved self-centering, but the maximum displacements were not reduced.

### *1.2. Aims and scope of the research*

The aim of the presented research is to investigate the effectiveness of centralized semi-active control approaches in reducing the maximum deformations and forces in post-tensioned steel frames under severe earthquake excitations.

Two centralized control systems are studied: (1) stiffness control approach (control of stiffness of the building during the earthquake to avoid dynamic amplification) and (2) deformation regulation approach (control of inter-story drifts to achieve uniform drift distribution along the height of the building).

Stiffness control approach has previously been used, but only on dual frames [14, 22] and truss structures, by activating/deactivating braces or truss members [15]. The stiffness control used in this study is not only its first application on PT frames, but is also based on a novel stiffness selection algorithm, using frequency analysis of the input motion. The overall stiffness of the frame is changed on the basis of a frequency analysis of the input motion. The main difference between previous stiffness control approaches and the one proposed here is that the control decision (gain) is independent from the structural response (open-loop control). This control approach does not require monitoring (or prediction) of structural response (displacements or velocities), and can be used not only for PT frames, but for frames with other structural configurations, including variable stiffness devices installed in brace-frame connections [12, 13].

Deformation regulation is a displacement-feedback approach that has been used for optimization of the seismic response of buildings [23], but never as a semi-active control strategy. The aim of this control approach is however not to reduce all displacements of the structure as this reduction may require stiffening the frame and increase the base shear during the earthquake. The deformation regulation approach employs the idea of equalizing the inter-story drift of all stories (equalizing strength/demand ratios) so that the base shear of the frame can be reduced [23].

## 2. MODEL FOR SIMULATING MOMENT-ROTATION BEHAVIOUR OF PT CONNECTIONS

Post-tensioned connections with energy dissipaters are characterized by flag-shaped hysteretic behaviour (Figure 1, [2]). After experiencing inelastic deformations in the energy dissipater the connection returns to its original position due to the effect of post-tensioning forces.

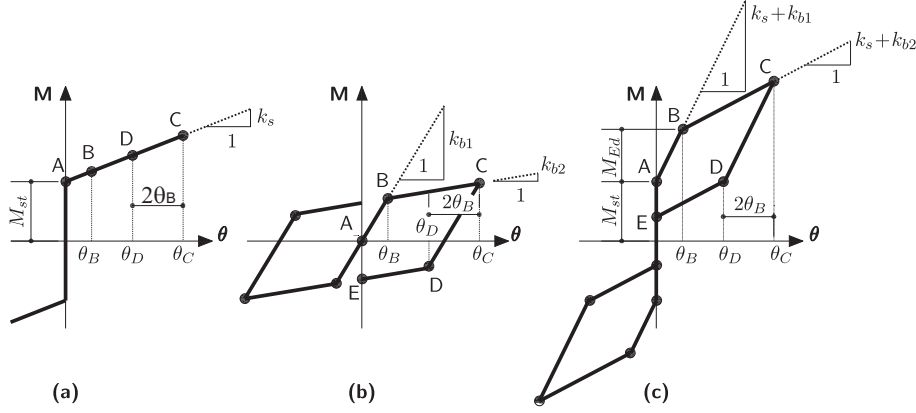


Figure 1. Hysteretic model for post-tensioned connection with energy dissipating bars [2]: (a) post-tensioned strands, (b) energy dissipating bars and (c) post-tensioned connection (combined action).

The moment-rotation behaviour of post-tensioned steel connections with bi-linear energy dissipaters can be described for different phases of loading (Figure 1). As long as the applied moment is less than the moment provided by the post-tensioned strands ( $M_{St}$ ), the connection behaves as a rigid connection experiencing no relative rotations between the beam and the column. When the applied moment exceeds  $M_{St}$ , a gap opens between the beam and the column and the energy dissipating device starts contributing to the resisting moment of the connection. In this stage (A-B) the resisting moment of the connection can be calculated from:

$$M_{A-B} = M_{St} + (k_s + k_{b1})\theta, \quad (1)$$

where  $k_s$  is stiffness of the strands,  $k_{b1}$  is pre yielding/slipping stiffness of the energy dissipater, and  $\theta$  is the angle of rotation between the column and beam.

When the applied moment exceeds the yield/slip force of the energy dissipater (stage B-C), the resisting moment of the connection is:

$$M_{B-C} = M_{A-B} + (k_s + k_{b2})(\theta - \theta_B), \quad (2)$$

where  $k_{b2}$  is the second, post-yield stiffness of the energy dissipating device and  $\theta_B$  is the rotation angle at which the energy dissipating device starts yielding/slipping. If the energy dissipating device is friction based, the second stiffness is zero.

The unloading of the connection is characterized by two stages. The first stage (C-D) takes place when  $\theta_D \leq \theta \leq \theta_C$ , where  $\theta_D = \theta_C - 2\theta_B$ . The resisting moment of the connection in this stage is:

$$M_{C-D} = M_{B-C} + (k_s + k_{b1})(\theta - \theta_C), \quad (3)$$

The second unloading stage (D-E) starts when  $\theta \leq \theta_D$  and the resisting moment can be obtained from:

$$M_{D-E} = M_{C-D} + (k_s + k_{b1})(\theta - \theta_D), \quad (4)$$

The effects of the energy dissipating device on the moment-rotation behaviour of the connection can be described by the energy dissipation factor  $\beta$ . This factor shows the contribution of the energy dissipating device to the moment capacity of the connection:  $\beta = M_{Ed}/M_{St}$ , where  $M_{Ed}$  is moment

provided by the energy dissipation device and  $M_{St}$  is moment provided by post-tensioned strands before opening the gap.

The values of  $\beta$  lie within the range  $[0,1]$ . When  $\beta = 0$  the system is bi-linear elastic. The upper limit of  $\beta$  is imposed by the requirement of full self-centring of the connection (Figure 2). For higher values of  $\beta$  (or lower values of post-tensioning forces), the connection experiences residual rotations. Christopoulos et al. [6] showed that for energy dissipating devices with bi-linear elasto-plastic behaviour, the full self-centring requirement is satisfied when:

$$M_{St} \geq (k_{b1} - k_{b2})\theta_B \quad (5)$$

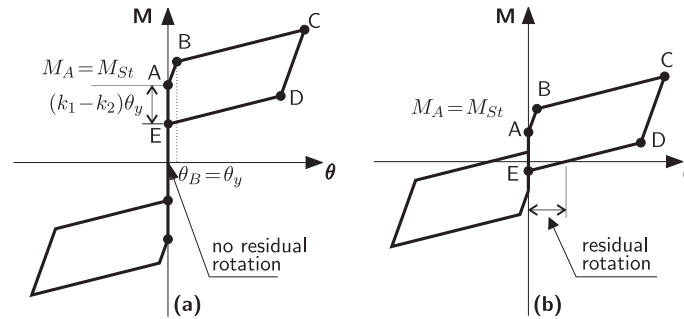


Figure 2. Illustration of the full self-centring requirement: (a) sufficient post-tensioning forces and (b) insufficient post-tensioning forces.

### 3. SEMI-ACTIVE CONTROL OF PT FRAMES USING STIFFNESS CONTROL APPROACH

#### 3.1. Basics of stiffness control approach

The purpose of the stiffness control approach is to control the natural frequency of the frame in order to avoid exciting the structure at one of the major frequency components of the earthquake. This concept was first proposed by Kobori et al. [14] who used active variable stiffness systems to control the seismic response of a three-story braced frame. Here, this concept is applied to control the dynamic response of post-tensioned frames using the characteristics of post-tensioned connections.

Moment-rotation relationship of post-tensioned beam-column connections naturally supports the stiffness control approach as it is composed of several phases of response with different loading stiffness, which can be controlled by the value of the PT forces in the connections. The number of loading stiffness values in the moment-rotation relationship of the connection depends on the energy dissipating device installed in the connection (Figure 3). Post-tensioned connections with friction based dissipation mechanism have two stiffness values (pre-slippage and post-slippage). Post-tensioned connections with energy dissipating bars have three stiffness values: pre-gap opening, between gap opening and bars yielding, and post bars yielding. Post-tensioned connections with top and seat dissipating angles have more than three stiffness values based on the number of plastic hinges forming in the dissipating angles (usually three plastic hinges) [1].

During earthquake excitations, the stiffness of the connection varies depending on the level of loading. At any time, the current stiffness of all connections in the frame governs the tangent stiffness of the frame. By varying the post-tensioning forces of each story, the gap-opening moment can be controlled, the total stiffness of the frame can be adjusted and the natural frequencies of the frame can be shifted to avoid exciting the frame at the frequencies of modes with high modal mass participation factors.

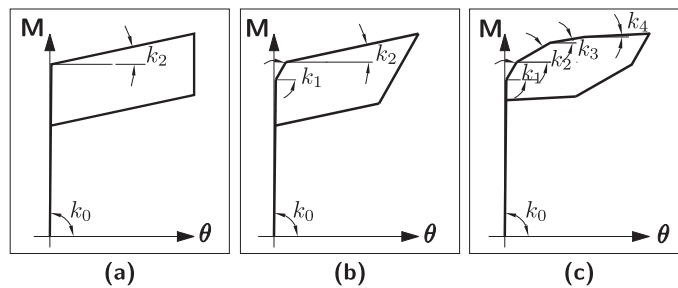


Figure 3. Stiffness values for post-tensioned connections with different energy dissipation mechanisms: (a) friction-based energy dissipation, (b) energy dissipating bars and (c) top and seat energy dissipating angles.

### 3.2. Frequency state feedback control algorithm (FSFA)

The aim of the frequency state feedback control algorithm (FSFA) is to alter the stiffness of post-tensioned frames so that the natural frequency is shifted away from the predominant frequencies of the earthquake. This is performed by analyzing the frequency content of the exciting earthquake at regular time intervals. The length of these time intervals is pre-set and used as an input parameter for the control algorithm.

The first step in the FSFA is to determine all stiffness patterns of the frame, which are the available control options for the frame. For instance, if beam-column connections in the frame are yield-based with energy dissipating bars, each story can take three stiffness values  $k_0$ ,  $k_1$  and  $k_2$  (Figure 3-b). Load and deformation ranges for  $k_1$  are small compared to  $k_0$  and  $k_2$ , respectively, and therefore  $k_1$  is not taken into account in the algorithm, and the number of controlled stiffness patterns is reduced to 2 per story. Thus, a stiffness pattern is a vector with  $N_s$  number of elements, where each element can take the value of  $k_0$  or  $k_2$ . The total number of stiffness patterns in the frame is  $S = 2^{N_s}$ , where  $N_s$  is number of stories in the frame. The same vector of stiffness patterns can be used if the frame is provided with friction-based connections or post-tensioned connection with top and seat angles.

Modal analysis is then performed for each stiffness pattern to determine natural frequencies ( $f_i$ ) and modal mass participation ratios ( $\Gamma_i$ ). In this study only the first and the second mode of vibration were included in the algorithm. As a result, stiffness patterns matrix is assembled as illustrated in Table I. It should be noted that these steps of the algorithm are independent from the seismic excitation.

Pattern	Story Stiffness				Modal Frequencies		Modal Mass Participation Factors	
	1 <sup>st</sup> Story	2 <sup>nd</sup> Story	...	$N_s^{th}$ Story	1 <sup>st</sup> Mode ( $f_{i,1}$ )	2 <sup>nd</sup> Mode ( $f_{i,2}$ )	1 <sup>st</sup> Mode ( $\Gamma_{i,1}$ )	2 <sup>nd</sup> Mode ( $\Gamma_{i,2}$ )
1	$k_0$	$k_0$	$k_0$	$k_0$	$f_{1,1}$	$f_{1,2}$	$\Gamma_{1,1}$	$\Gamma_{1,2}$
2	$k_2$	$k_0$	$k_0$	$k_0$	$f_{2,1}$	$f_{2,2}$	$\Gamma_{2,1}$	$\Gamma_{2,2}$
...	...	...	...	...	...	...	...	...
S	$k_2$	$k_2$	$k_2$	$k_2$	$f_{S,1}$	$f_{S,2}$	$\Gamma_{S,1}$	$\Gamma_{S,2}$

Table I. Assembly of the stiffness patterns matrix.

The FSFA is applied at regular time intervals with a pre-set length ( $T_c$ ), which is an input parameter in the algorithm. During the control interval, the FSFA acquires the accelerations at the base of the structure (earthquake input). Once the control interval is completed, the recorded time-history (at  $t = mT_c$ , where  $m$  is the number of previous control intervals) is analyzed using Fourier Transform (in this case FFT) to find the frequency content of the excitation.

The result of the FT is an amplitude spectrum of ground acceleration which is then used to compute the correlation between the frequency content of the excitation and the response amplitudes

at the first two natural frequencies of all stiffness patterns of the structure. The correlation is quantified by using a frequency response index ( $FR_i$ ) calculated as a sum of the products of the spectral amplitudes at the frequencies of the first two modes of each stiffness pattern and their corresponding modal mass participation factors:

$$FR_i = \Gamma_{i,1}\Psi_{i,1} + \Gamma_{i,2}\Psi_{i,2}, \quad (6)$$

where  $FR_i$  is the frequency response index of the  $i^{th}$  stiffness pattern,  $\Gamma_{i,1}, \Gamma_{i,2}$  are effective modal mass participation ratios for the first and second mode of vibration of the  $i^{th}$  stiffness pattern and  $\Psi_{i,1}, \Psi_{i,2}$  are the spectral acceleration amplitudes of the first and second modes of vibration of the  $i^{th}$  stiffness pattern. The calculation of  $FR_i$  is illustrated in Figure 4.

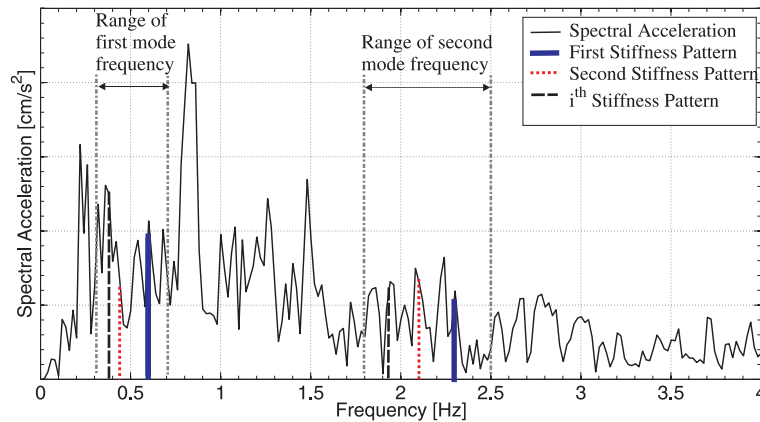


Figure 4. Computation of frequency response index for different stiffness patterns and a given amplitude spectrum of ground acceleration.

The control algorithm adjusts the stiffness in the connections at each floor level to achieve the stiffness pattern with the minimum value of  $FR$ . When the story stiffness for the required pattern is  $k_0$ , post-tensioning forces in this story are increased (strands are tightened) to the pre-set upper limit (in this case about 70% of the yielding force of the strands). When the required story stiffness is  $k_2$ , the post-tensioning forces in the story are reduced (strands are released) to the lower limit, which satisfies the requirement for self-centring of the connection given in Equation 5.

After every control time interval ( $T_c$ ), the amplitude spectrum of the excitation is updated, and the operation of the algorithm is repeated. In this procedure the excitation is represented by a cumulative spectrum. Alternatively, Fourier spectra can be calculated segment-by-segment, or by overlapping segments, which would give a better representation of the current frequency content of the excitation. The main reason for using the cumulative acceleration history for the Fourier transform was to reduce the influence of sudden changes in the frequency content of the seismic input on the performance of the control system. This means that in this case the calculation of the frequency content is inaccurate in the initial control intervals, but the accuracy improves in the following steps. The process of updating the amplitude spectrum at three successive control intervals is shown in Figure 5. It should be noted that the FSF control algorithm is not activated until the completion of the first control interval, during which the initial stiffness pattern is  $k_0$  in all stories (the stiffest possible case).

The selection of the control time interval ( $T_c$ ) is a procedure which depends on type of the earthquake, structural characteristics and power of the rotating motor used in the control system. Longer  $T_c$  can be used for far field earthquakes, where the high frequency components have been eliminated [29]. Near field earthquakes, characterized by sudden changes in frequency content, require shorter  $T_c$  to achieve good control. In this study  $T_c = 3s$  was adopted to allow acquiring 128 data points (at sampling rate of 50 samples/s), required for Fourier spectrum in the range of 3.38 Hz.

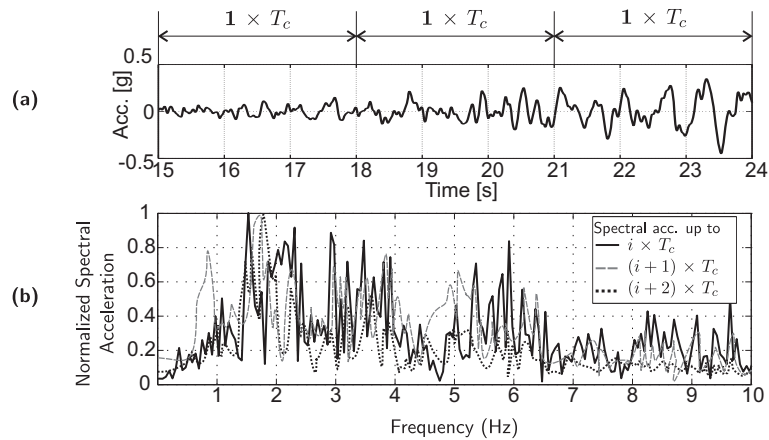


Figure 5. Updating of the amplitude spectrum of excitation in three successive control intervals ( $T_c = 3$ s), Northridge 1994: (a) ground acceleration, and (b) Fourier amplitude spectrum of acceleration.

Since the input data for the Frequency State Feedback Algorithm (FSFA) are only the accelerations of the excitation, this algorithm is an open-loop feedback control algorithm, where the structural response is not included. Hence, the operation of the control algorithm and the control gains depend only on the analysis of the earthquake input.

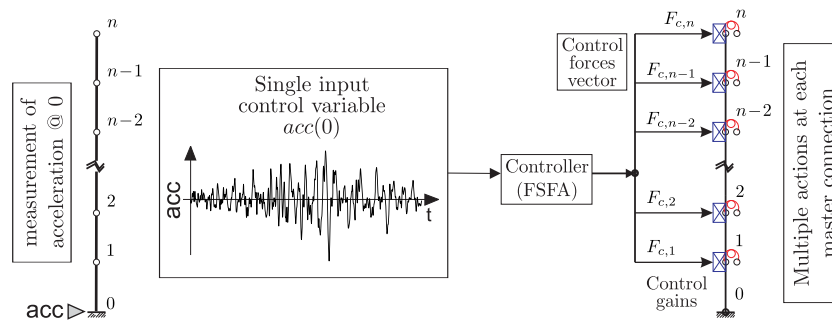


Figure 6. Operation of stiffness-based control algorithms as SIMO systems.

Structures with stiffness-based control algorithms can be considered as Single-Input-Multi-Output systems (SIMO). The input of the control algorithm is one measurement which can be acceleration of the earthquake or the response acceleration, whereas the outputs are control forces acting at each story (Figure 6). Although the control gains could be different for different storeys, they are all combined in one vector which is the output of the controller. Therefore, the output of the controller is not a set of  $n$  independent values but a single vector representing the selected stiffness pattern. The next step is assembling the control gains vector comprising  $n$  values, each calculated as a difference between the current forces and the ones required by the selected stiffness pattern. The flowchart of the algorithm is shown in Figure 7. The main characteristics of the FSF control are compared to those of the two existing stiffness control algorithms in Table II.

#### 4. SEMI-ACTIVE CONTROL OF PT FRAMES USING DEFORMATION REGULATION APPROACH

##### 4.1. Basics of deformation regulation approach

The deformation regulation approach is based on controlling and redistributing the structural deformations over the height of the structure. The aim is to avoid concentrated response (large

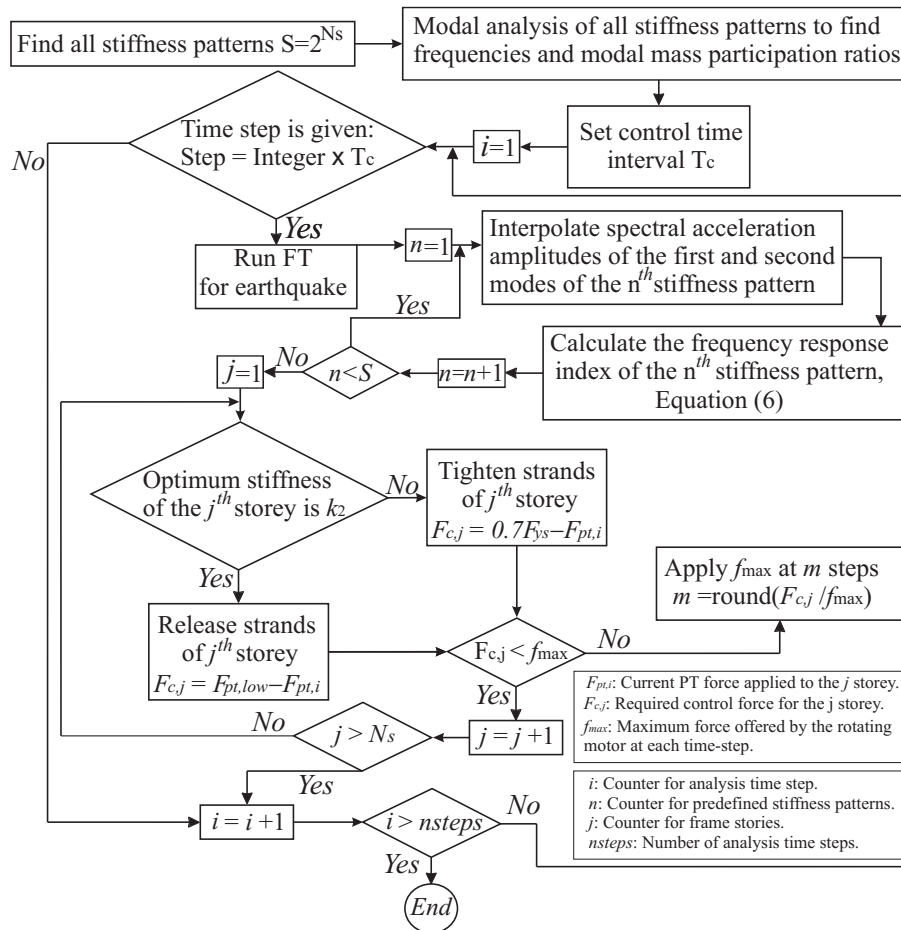


Figure 7. Flowchart of the excitation frequency state feedback control algorithm.

	AVS	MET	FSF
<b>Type of structure</b>	multi-story dual frame	truss structure	multi-story PT frame
<b>Control action</b>	activate - deactivate braces	activate - deactivate additional members	change PT forces
<b>Measured parameter</b>	response acceleration history	response displacements and velocities	input acceleration history
<b>Stiffness selection criteria</b>	indices obtained in parametric studies	minimizing total modal energy	Fourier spectrum of input acceleration
<b>Control system</b>	close-loop	close-loop	open-loop

Table II. Comparison between Frequency State Feedback (FSF) and other stiffness control algorithms: (AVS) Active variable stiffness [12], (MET) Modal energy transference [13].

inter-story displacements) at some stories of the structure, while other stories are less affected. This can cause concentration of internal forces, damage in a limited number of structural elements and eventually lead to a soft story mechanism.

In a well-designed multi-story structure, the ratios between strength and demand (over-strength ratios) in the elements are supposed to be distributed evenly over all storeys. However, this is not achievable for passively controlled systems as the response of a structure depends also on the properties of the earthquake excitation. Therefore, the deformation regulation approach aims at

rearranging the internal forces in the elements in the structure (resistance), so that the over-strength ratios are evenly distributed, regardless of the properties of the earthquake excitation.

#### 4.2. Uniform Drift Distribution Algorithm (UDDA)

In this control algorithm, the post-tensioning forces are redistributed over the frame in order to regulate the peak values of inter-story drift. The aim is to provide an even distribution of all inter-story drifts so there is no concentration in internal forces in one story.

The first step in this control algorithm is determining the drift threshold at which the algorithm is activated. The drift threshold  $\eta_{th,i}$  is defined for each floor, as a ratio of story height, and used as input in the algorithm.

The operation of the UDDA is in three stages: (i) activation, (ii) control action, (iii) deactivation.

(i) Activation: The algorithm is activated whenever the following two conditions are satisfied: (a) any of the inter-story drifts has exceeded the threshold  $\eta_{th,i}$ , and (b) at least one inter-story drift has reached a peak value. Whenever an inter-story drift exceeds the threshold, the algorithm starts assembling a column vector (PeakCode). The value of the PeakCode vector for each story is 0 if the story drift has not reached a peak or 1 if it has reached a peak. The algorithm is activated when at least one of the PeakCode values becomes 1.

(ii) Control Action: When the control algorithm is activated, the average of all inter-story drifts is calculated in each response time step. For stories with inter-story drifts less than the average value, the post-tensioning forces are decreased (strands are released). For stories with inter-story drifts higher than the average value, the post-tensioning forces are increased (strands are tightened). The amount of increase or decrease of post-tensioning force in  $j^{th}$  story is:

$$F_{c,j} = \frac{D_j - D_{av}}{D_{av}} \times F_{pt,j}, \quad (7)$$

where  $F_{c,j}$  is the control force that needs to be applied to reach the desired PT force,  $D_j$  is inter-story drift,  $D_{av}$  is average of the inter-story drifts at all storeys, and  $F_{pt,j}$  is post-tensioning force applied to the story, all recorded at the moment of activation. Control force  $F_{c,j}$  is applied at a rate determined by the characteristics of the rotating motor [21], which means that a period of time is needed to complete the control action. If a new activation event occurs during this time, the control action is interrupted and the algorithm starts a new control sequence (new control forces are calculated).

(iii) Deactivation: If the control action is completed (desired PT forces are achieved), and all values of the PeakCode vector are 0, the algorithm is deactivated and PT forces remain unchanged until the algorithm is activated again.

As the input data of the control algorithm are only the inter-story drifts of the frame, and the properties of the excitation do not affect the algorithm outputs, the UDDA can be classified as a close-loop control algorithm. The operation of UDDA is illustrated in Figure 8.

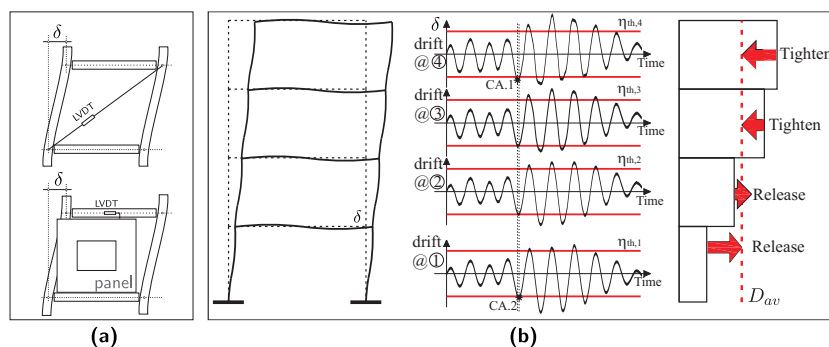


Figure 8. Uniform Drift Distribution control Algorithm (UDDA): (a) possible solutions for measuring drift, (b) illustration of the operation of UDDA (CA.1: activation of the algorithm, CA.2: new control forces calculated before completion of CA1 sequence).

The UDDA can be considered a Multi-Input-Multi-Output system (MIMO) where input data (input variables) are the inter-story drifts (a vector of multiple elements) and the output data (control gains) of the algorithm is a vector of control forces which also comprises multiple elements (Figure 9). Figure 10 shows the flowchart of the operation of the Uniform Drift Distribution control algorithm.

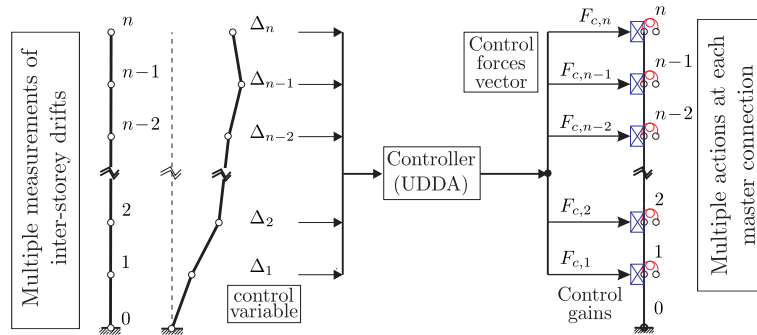


Figure 9. Operation of the UDDA as MIMO systems.

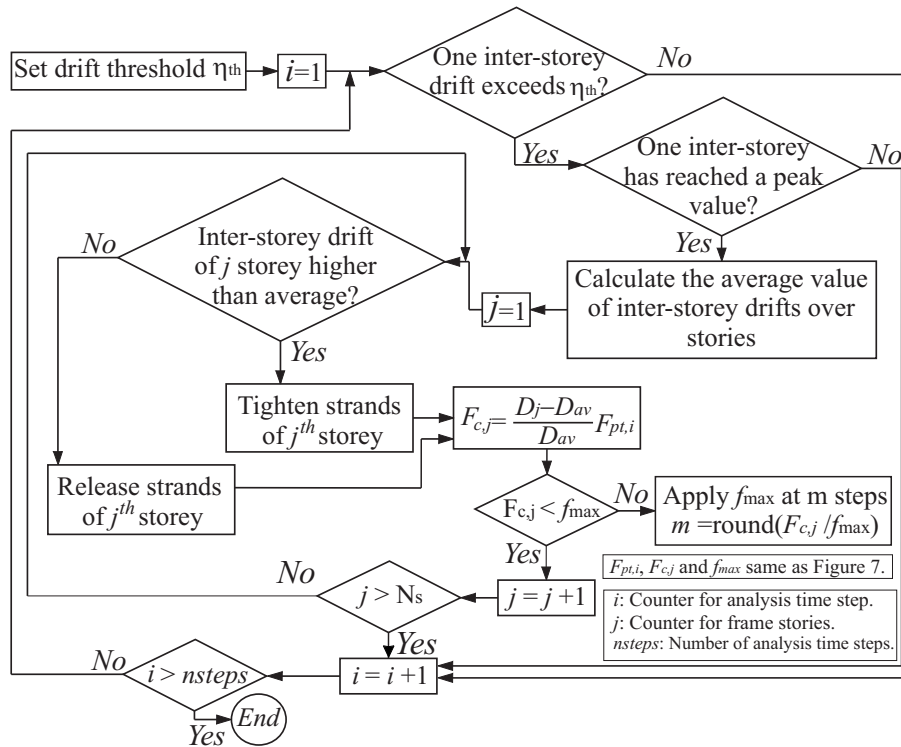


Figure 10. Operation flowchart of the uniform drift distribution control algorithm (UDDA).

## 5. SIMULATION OF RESPONSE OF PT FRAMES WITH CENTRALIZED SEMI-ACTIVE CONTROL

### 5.1. Frame model

The effectiveness of the two new control strategies (FSFA and UDDA) was examined on a six-story one-bay frame (Figure 11). Each story is assumed to be equipped with a rotating motor

for controlling the post-tensioning forces in strands (installation details shown in Figure 12). The specifications of the motor (Figure 12) were selected from a list of commercially available units.

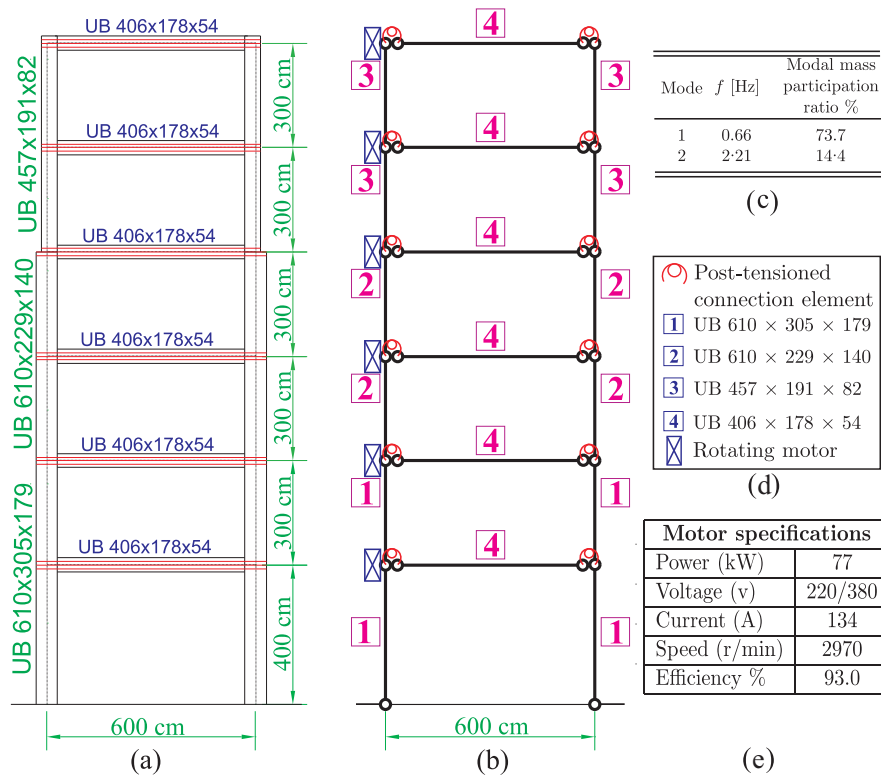


Figure 11. Six-story post-tensioned steel frame: (a) frame geometry and sections, (b) idealized model of the frame, (c) modal properties of the PT frame, (d) element and section properties and (e) specifications of rotating motors.

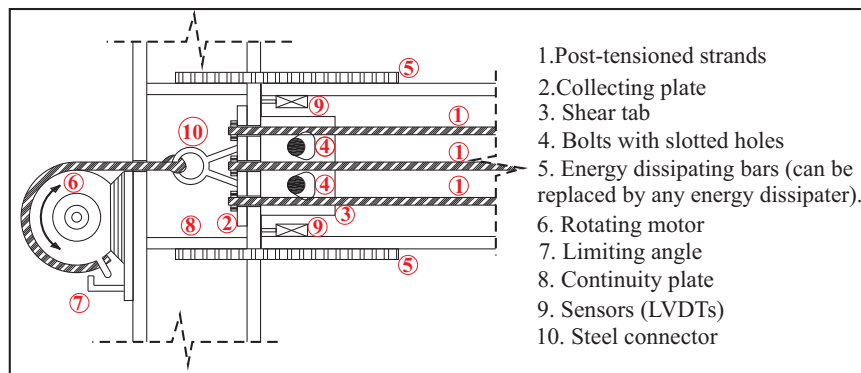


Figure 12. Arrangement of external post-tensioned connection equipped with system for controlling the strands forces.

The post tensioned frame was designed in accordance with the capacity design principles specified in Eurocode 8 [24], for ductility class  $H$ , by assuming the following damage sequence: (1) inelastic deformations in the connection (yielding/slip of dissipaters), (2) plastic hinges at the base of columns, (3) plastic deformations in beams under combined axial load and moment, (4) hinges in columns (above base) and (5) failure of connection (yielding of strands). The assumed damage hierarchy complies with that proposed by Garlock et al. [4] using the performance-based

design [25] of post-tensioned frames. In order to achieve plastic deformations under moments and axial forces in the beams, they are assumed to be laterally restrained elements made of class 1 sections [26].

The PT connection is represented by a single rotational spring model [27]. This model is simple to implement in a frame analysis and results in a global response of the frame similar to that obtained by using multi-element discrete springs models [28]. Simulations of the seismic behaviour of the passive and semi-active control of PT frames were performed using FASAC-2D (Frame Analysis with Semi-Active Control, [29]), a new computer program developed specifically for this purpose.

The initial post-tensioning forces were taken as 300 kN (about 30% of strands yield force; referred to as *low initial PT force*), which remained constant in the passive system and were varied by the semi-active control algorithms, when the semi-active control was applied. The modal properties of the passive frame for the first two modes are presented in Figure 11-c. As the modal properties of the PT frame are calculated for the linear-elastic system (no gap opening or yielding in energy dissipating elements), they are the same for the passive frames with both low and high PT forces.

## 5.2. Earthquake excitations

The post-tensioned frame was analysed through simulations of non-linear response to a set of scaled earthquakes (Table III and Figure 13, [30]).

Earthquake	Year	Country	Record	$\Delta t$ (sec)	Duration (sec)	Spectrum*; PGA
El-Centro	1940	USA	IMPVALL/I-ELC180	0.020	53.760	S1; 0.5g
Borrego Mountain	1968	USA	BORREGO/A-ELC180	0.010	40.000	S2; 0.2g
Tabas	1978	Iran	TABAS/BAJ-V1	0.020	39.400	S1; 0.5g
SMART1	1983	Taiwan	SMART1/25C00EW	0.010	24.000	S2; 0.2g
Mexico-City	1985	Mexico	MEXICO-SCT1-021	0.020	180.000	– ; 0.1g
Erzikan	1992	Turkey	ERZIKAN/ERZ-NS	0.005	21.325	S2; 0.2g
Landers	1992	USA	LANDERS/H05000	0.02	56.000	S1; 0.5g
Northridge	1994	USA	NORTHR/HOS090	0.01	40.000	S1; 0.5g

Table III. Details of earthquake records (\*Scaling spectra shown in Figure 13)

The selected earthquake records provide a wide range of characteristics such as: (i) frequency content, (ii) intensity and (iii) distribution of large amplitudes over the earthquake duration (shape of the earthquake envelope; [31]), which is one of the factors that affects the performance of the system. Therefore, the earthquake records were not scaled as recommended by Somerville et al. [32]. Instead, acceleration amplitudes were scaled to PGA levels (Table III) that produced nonlinear behaviour of the structure and resulted in response similar to that under design-based earthquakes (DBEs, [25]), determined as maximum inter-story drift of at least 1.5% [33].

## 5.3. Results of FSFA control

**5.3.1. Frame response.** Top story displacements obtained by using the FSFA control with control time interval ( $T_c = 3s$ ) are presented in Figure 14, together with displacements obtained for a passive frame with low PT forces. These results show that the FSFA reduced the maximum displacements under all excitations, in most cases (Mexico City, El Centro, Tabas, Smart, Landers) significantly.

The largest reduction in top story displacements is noticed for the Mexico City earthquake. The large reduction can be explained by the difference in spectral amplitudes of the earthquake acceleration (Figure 15-a) at the frequencies of the first mode of the passive frame (prior to gap-opening) and the first mode of the final stiffness pattern of the FSFA-controlled frame. The change

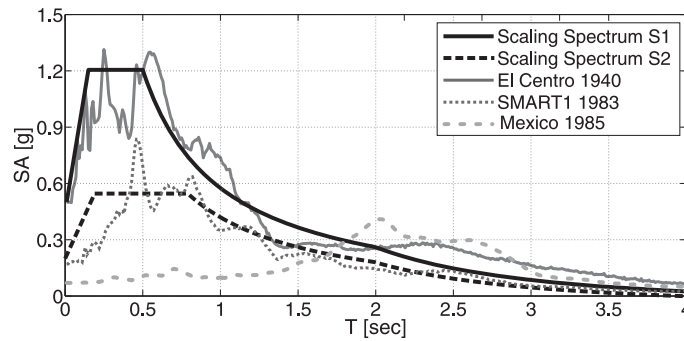


Figure 13. Selected earthquakes response spectra.

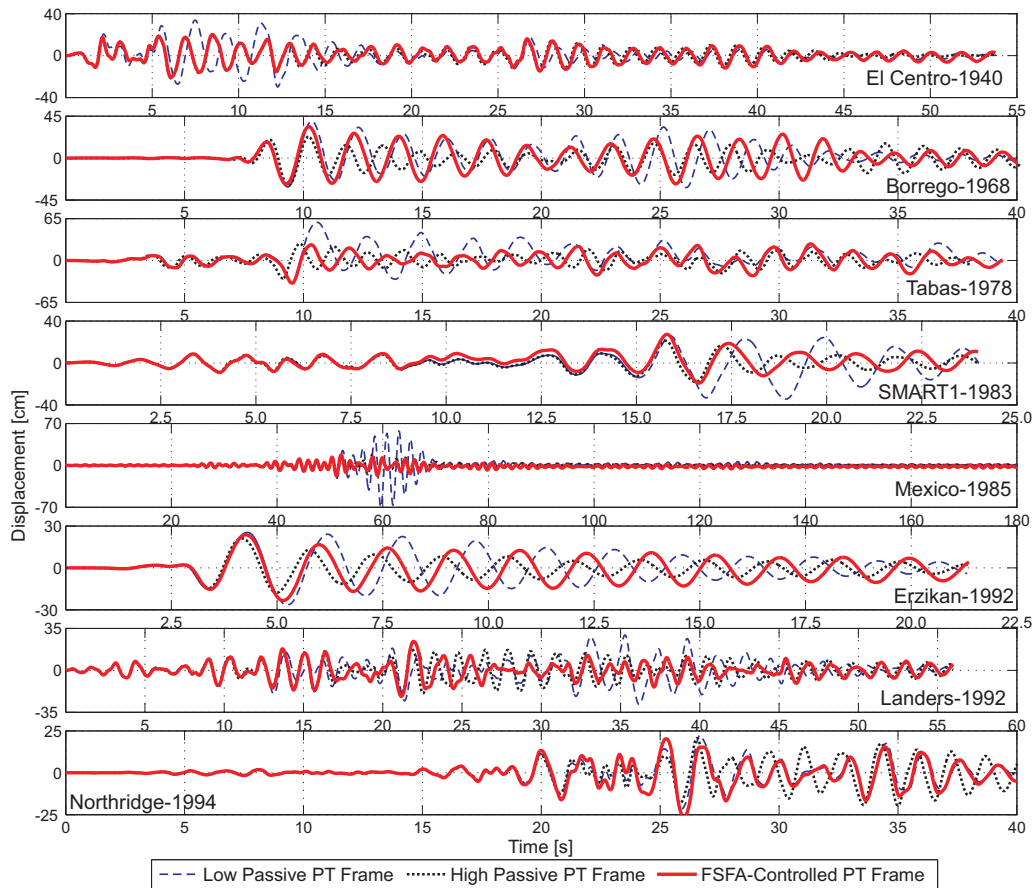


Figure 14. Top story displacements for passive and FSFA-controlled PT frames.

in stiffness patterns is illustrated in Figure 15-b showing the change in the first and second mode frequencies, as the controller changes the stiffness patterns during the earthquake action.

The diagrams of resultant PT forces of the FSFA-controlled frame at the end of the eight applied earthquake excitations is shown in Figure 16. The distribution of PT forces along the height shows the final stiffness pattern of the building after the earthquake action: if the final PT force at a story is lower than the initial PT force (Low Passive Force  $F_{pt,1}$ ), the story stiffness is  $k_2$ ; if it is higher than  $F_{pt,1}$ , the stiffness is  $k_0$  (initial stiffness). In Figure 16 are shown the numbers of the final stiffness patterns and the corresponding frequencies of their first and second modes of vibration, for each earthquake.

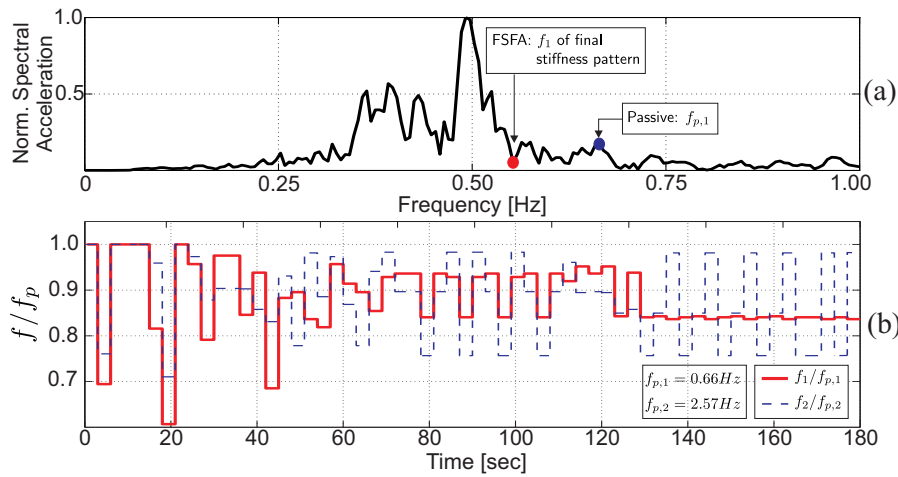


Figure 15. (a) Frequency content of Mexico earthquake with first mode frequency of passive and controlled frames and (b) Variation of the first and second mode frequencies in the controlled frame under Mexico City earthquake;  $f_{p1}$ : first mode frequency of the passive frame,  $f_{p2}$ : second mode frequency of the passive frame.

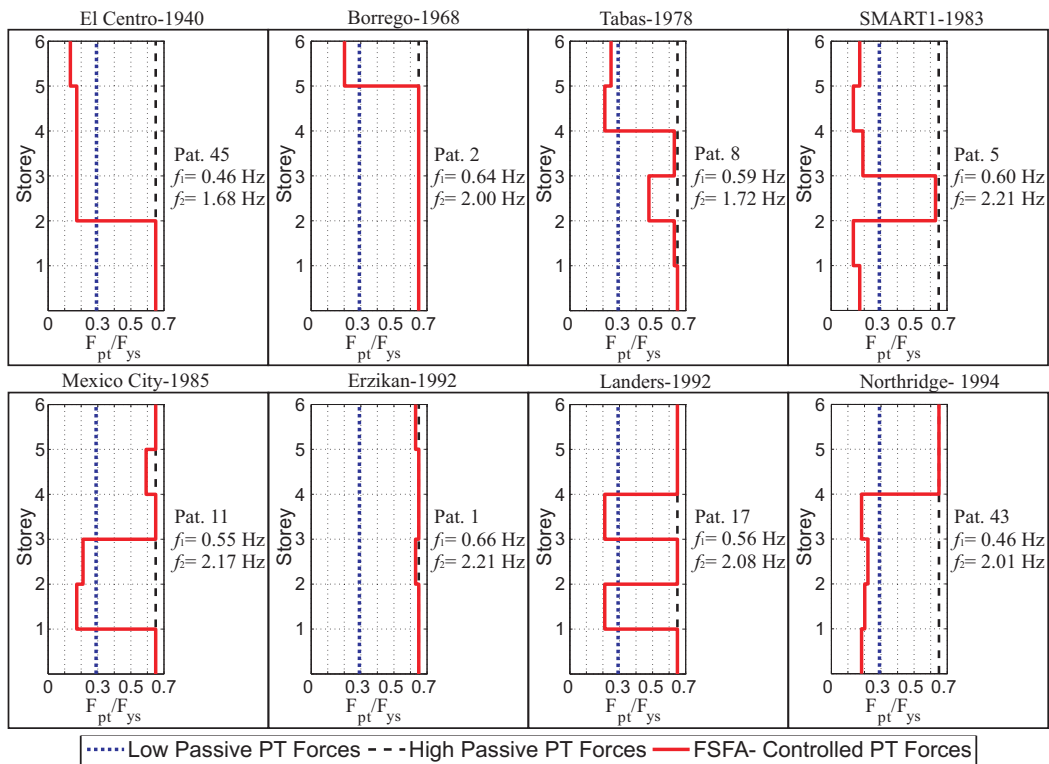


Figure 16. Distribution of PT forces (final stiffness patterns) in the FSFA-controlled frame at the end of the seismic actions.

The final PT force distributions (Figure 16) show that by using FSFA the PT forces reach the maximum allowed values of 70% of the strands yield force  $F_{ys}$ . Hence, the comparison between the responses of a frame with low passive PT forces and FSFA-controlled frame is not appropriate. The comparison between top story displacements of the FSFA-controlled frame and a passive frame with higher PT forces ( $F_{pt,1} = 0.7F_{ys}$ , Figure 14) shows that the maximum displacements of the two frames are similar. This means that the FSFA control maintains low displacements by employing

PT forces that are generally lower than these in the passive frame, in some cases even below the initial PT force of  $0.3F_{ys}$ . This leads to reduction in base shear and a reduction in the moment demand on connected columns. The largest reduction in resultant PT forces was noticed for El-Centro, SMART1 and Northridge earthquakes, during which the frame displacements were similar to those in the passive frame with high initial PT forces ( $0.7F_{ys}$ ).

It should be noted that applying high initial PT forces does not necessarily result in reduced displacements. When initial PT forces are too high, the stiffness of the frame remains high and the structure behaves elastically during a large part of the action. The PT frame in this case could be excited at the frequency of its first mode of vibration, leading to magnification of the seismic input. Figure 17 shows an example of negative effect of high PT forces in the latter stages of response to the Northridge earthquake.

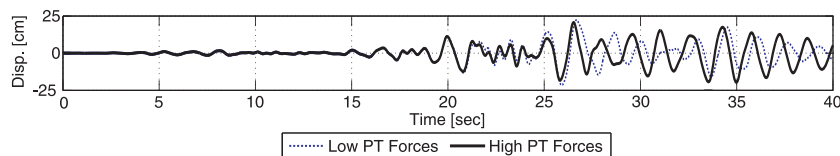


Figure 17. Example of negative effect of high initial PT forces on response: magnification at the end of the seismic action (Northridge excitation).

The predominant stiffness pattern of the frame during the earthquake is the one that is active most of the time. Figure 18 shows the histogram of the selected stiffness patterns, the distribution of PT forces for the predominant stiffness pattern and the frequency of its first mode of vibration. Pattern number 1 is identical to the passive frame, where all PT forces are equal to their initial values ( $0.7F_{ys}$ ). Similarly, pattern number 64 corresponds to a frame in which all PT forces are at the minimum value ( $F_{pt,low}$ ). The results in Figure 18 show a very different PT force distribution for different earthquakes: from keeping the initial stiffness throughout the seismic action (pattern No. 1, Erzikan), to a system in which low PT forces are maintained for most of the response (Landers and SMART1).

**5.3.2. Centralization of the FSFA.** The stiffness control using the FSFA is a centralized control approach in which one control action changes a property of the structure as a whole (i.e. natural frequency). In this approach, post-tensioning forces in different stories work together and form specific patterns of loading or unloading. The example in Figure 19, shows three successive stiffness patterns: (i) a mix of  $k_0$  and  $k_2$ , (ii)  $k_2$  in all stories (pattern 64) and (iii)  $k_0$  in all stories (pattern 1). When the required story stiffness is  $k_0$ , the PT forces are constant and kept at a level higher than the gap-opening force (in this case  $0.65F_{ys}$ ). When the story stiffness is  $k_2$ , the controller at that level increases-decreases the PT force by a pre-set increment/decrement, which depends on the motor capacity (in this case  $1000kN/s$ , resulting in  $20kN/step$ ) to maintain the force level at a prescribed  $F_{pt,low}$ .

The control force sets are synchronized as a result of one control action, such as "change stiffness pattern from pattern  $i$  to pattern  $ii$ ". This control action contains the required PT forces for all stories of the target stiffness pattern as well as the differences in PT forces between the current and required stiffness pattern.

## 5.4. Results of UDDA

**5.4.1. Frame response.** The UDDA control was applied by using low initial post-tensioning force ( $F_{pt} = F_{pt,low} = 0.3F_{ys}$ ) and varying the PT forces between this value and the upper force limit ( $F_{pt,high} = 0.7F_{ys}$ ). The results of the UDDA control simulations are compared with those obtained for two passive frames, one with low and one with high PT forces. The only other input parameter of the UDDA is the drift threshold ( $\eta$ ) which triggers the algorithm (if  $(D_i/h_i)_{max} \geq \eta$ , in this case  $\eta$  was taken as 0.005). A comparison of the top story displacement between the UDDA-controlled frame and the passive frame with low PT forces ( $F_{pt} = 0.3F_{ys}$ ) is presented in Figure 20. The results

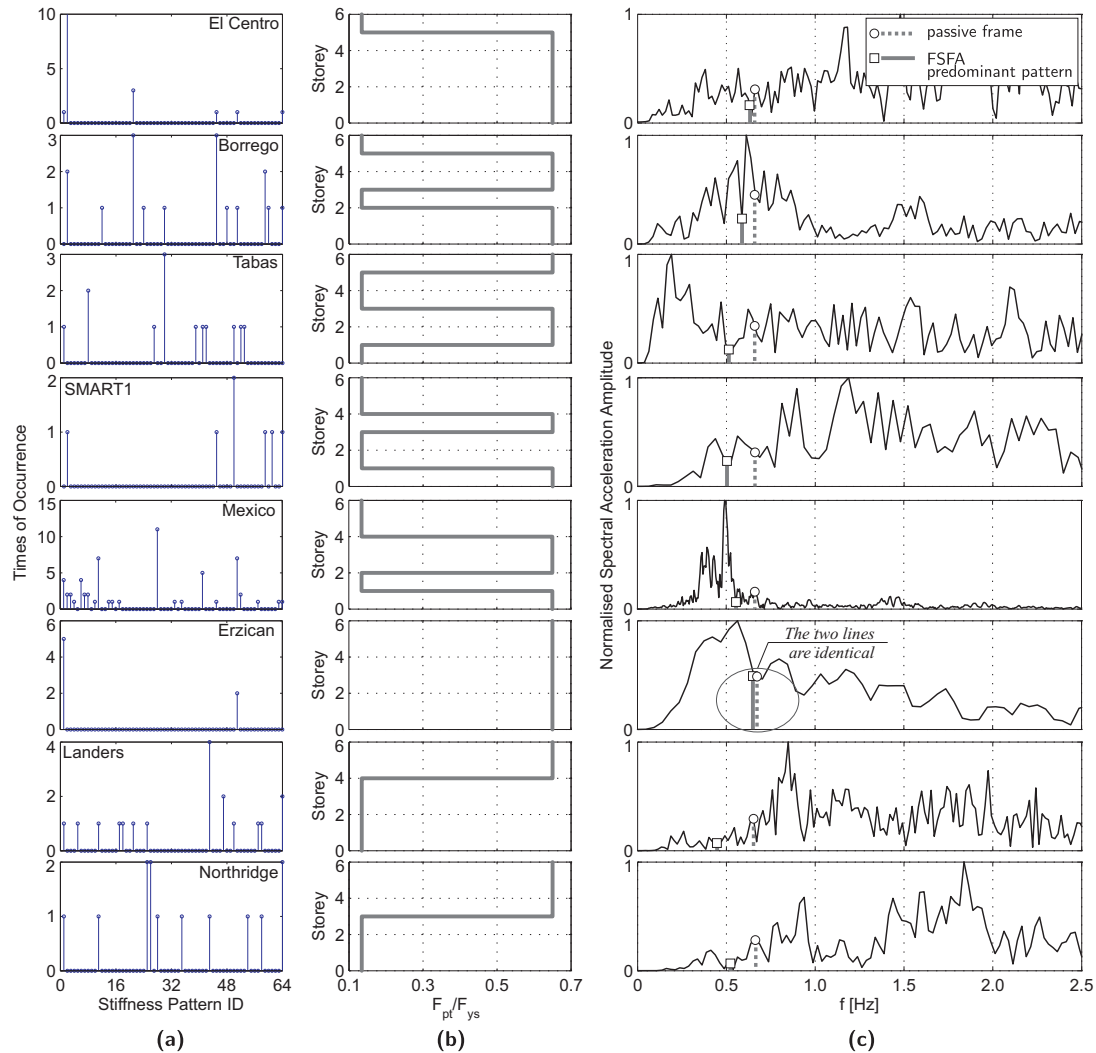


Figure 18. Predominant stiffness patterns of the frame for different earthquakes: (a) number of occurrences of stiffness patterns, (b) PT forces of the predominant stiffness pattern and (c) first mode frequency of the predominant stiffness pattern.

show that for two excitations (Erzican and Northridge) the top story displacements are similar for the two frames, with 30-40% reduction of the passive frame displacements under Borrego, Tabas and Landers and over 70% reduction in the case of Mexico City.

The diagram of PT forces at the end of the UDDA-control simulations (Figure 21) suggest that the first and the top story experience less inter-story drift than other stories and hence, the UDDA tends to reduce these PT forces in order to increase their inter-story drifts and equalize them with the drifts of the other storeys. The resultant PT forces show similar patterns for all earthquakes for this frame, but there are some differences in the final value of the resultant force.

Since the post-tensioning forces in the UDDA-controlled frame reach high level in some stories, comparison of the results between the UDDA-controlled frame and the passive frame with low initial PT forces is not appropriate as it compares two frames with different levels of post-tensioning. In order to obtain a better comparison, the maximum post-tensioning forces reached when applying the UDDA are applied as passive forces, constant for all storeys.

The comparison between the top story displacement of the passive frame with high forces ( $0.7 F_{ys}$ ) and the UDDA-controlled frame (Figure 20) show that the UDDA-controlled frame can achieve behaviour similar to the behaviour of a passive frame with high post-tensioning forces.

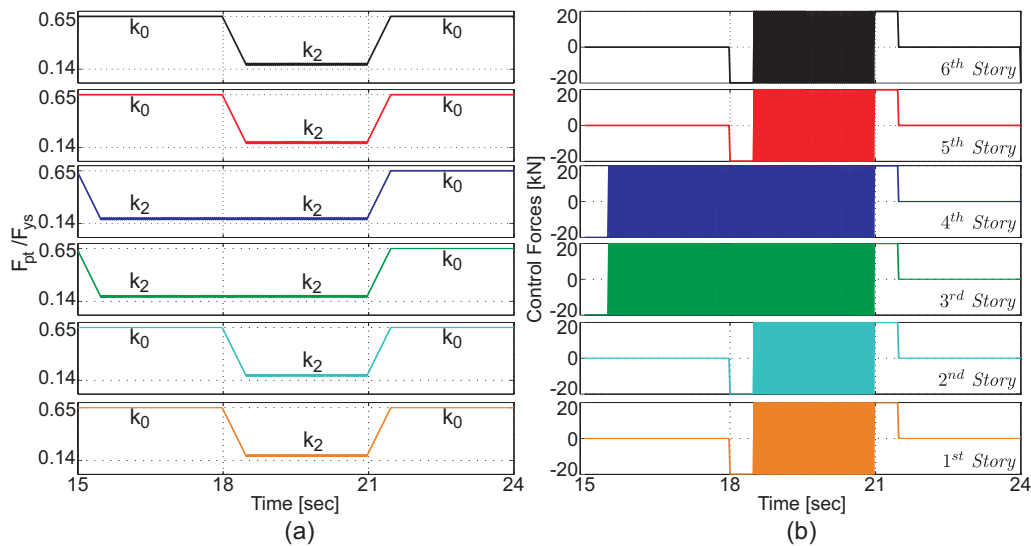


Figure 19. Centralization of control forces in FSFA: (a) PT forces and switching between  $k_0$  and  $k_2$  and (b) time-histories of control forces (input: Mexico City earthquake).

The reduction in the top story displacements of the UDDA-controlled frame is associated with a reduction in the moment demand on the columns of stories with low resultant PT forces. This means that a frame with UDDA can exhibit top story displacements similar to those in a passive PT frame with high post-tensioning forces but with reduced internal forces in some stories.

In addition to the good performance of the UDDA in controlling the top story displacement of the PT frame, differences in the maximum inter-story drift are also reduced when the UDDA is applied, which is the main objective of this algorithm. The standard deviation of these drifts (Figure 22) shows that UDDA results in a more uniform distribution of maximum inter-story drift of the frame, compared with both passive frames (with low and high PT forces). Even when the frame with low passive forces showed better distribution of inter-story drifts than the one with high passive forces (as in Erzikan earthquake); the UDDA-controlled frame showed even better distribution. These results show that the algorithm was able to achieve the control objective with PT forces lower than those in the passive frame with high PT forces.

**5.4.2. Centralization of UDDA.** When the UDDA is applied to a PT frame, every change in control forces of all stories is made by one action from the control computer. This control action is based on the position of all inter-story drifts at a given time. This is done by finding the average inter-story drift and modifying the post-tensioning forces in all stories accordingly. Since all control forces are given by one action, the UDDA is classified as centralized control algorithm. Control forces in this algorithm are synchronized for different stories (Figure 23). The control force histories (Figure 23) show that all sets of control forces start at the same time which indicates that all control forces act simultaneously. In the intervals where control forces are applied only to few storeys, the drifts in the other stories are close to the average drifts and no action is required by the algorithm.

## 6. DISCUSSION OF RESULTS

The results obtained with the two semi-active control approaches used in this research cannot be directly compared with all the results of previous studies. Most of the previous research on semi-active control is limited to linear systems, where the structure can be represented by a transfer function. These systems can be made highly effective by using Lyapunov stability [34], or quadratic regulators (linear [35] or non-linear [36, 37]), but cannot be used for structures that may develop non-linearity during earthquakes. Highly effective controllers based on fuzzy logic can be applied

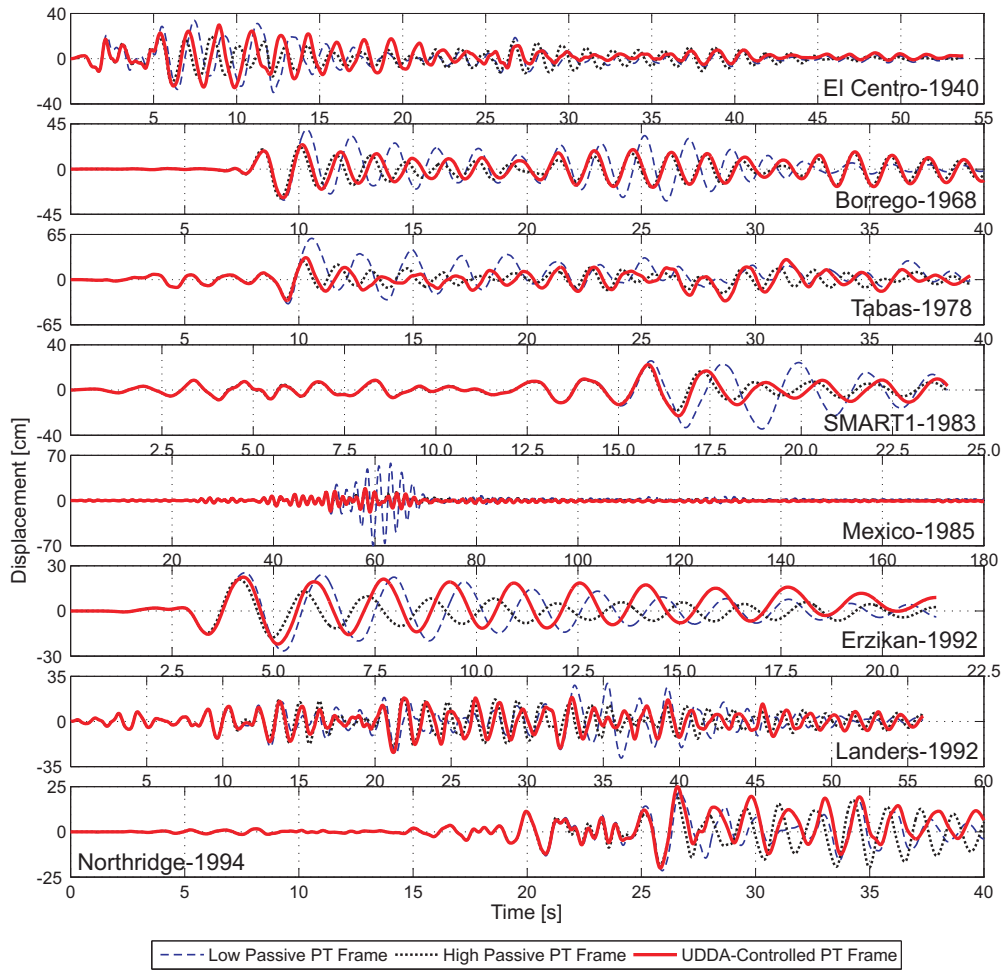


Figure 20. Top story displacements for UDDA-controlled and passive PT frames.

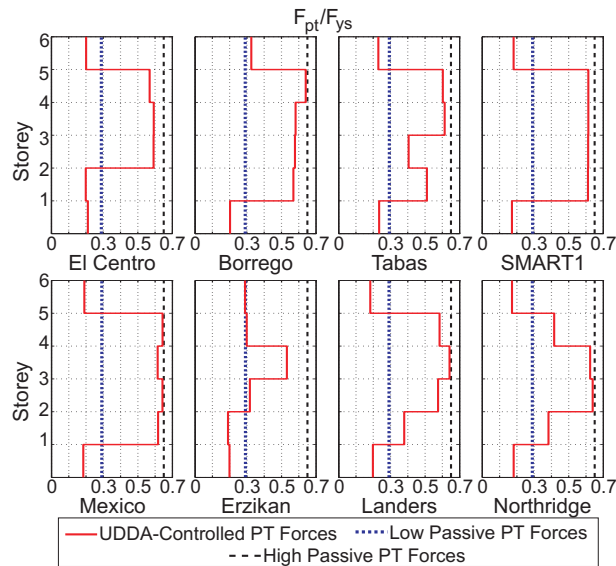


Figure 21. Resultant PT forces in UDDA-controlled frame.

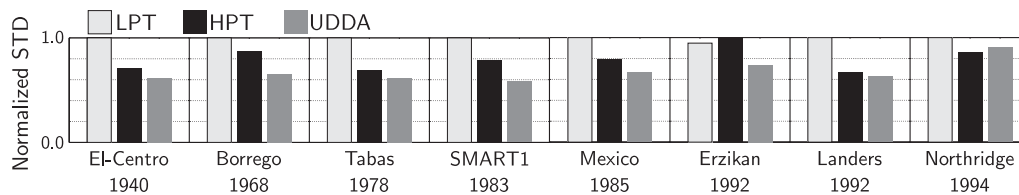


Figure 22. Standard deviations of the normalized inter-story drifts.

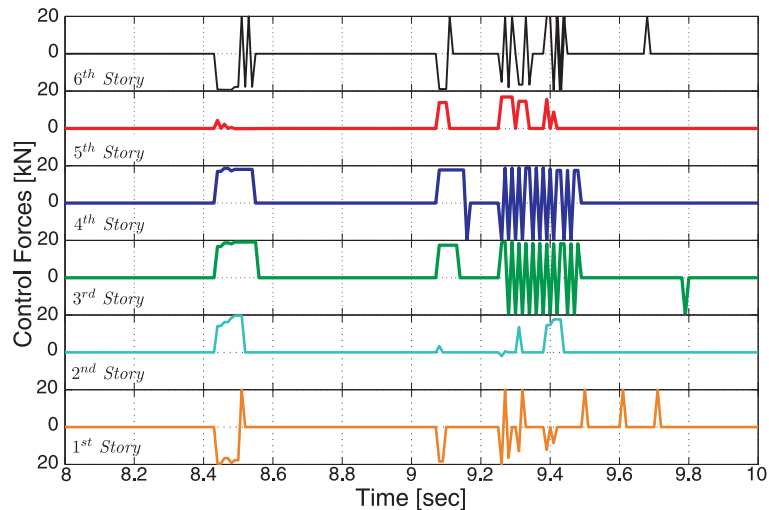


Figure 23. Control forces in UDDA.

to non-linear systems [38], but due to the complexities in determining the fuzzy functions [38, 39], this approach has only been used on simplified structures with maximum two dampers [40].

The stiffness control system (FSF algorithm) can be compared to the active variable stiffness system (AVS, [14]). FSFA shows similar reduction of displacements and accelerations to the AVS, when compared to the corresponding passive frames. In some cases, however, AVS resulted in large magnification in displacements due to “inappropriate stiffness selection” [14]. The performance of FSFA is comparable to that of controlled stiffness devices and friction dampers [13] applied on dual frames.

Hence, the best assessment of the efficiency of the semi-active control of PT frames is by comparison of the results with those obtained for the corresponding passive structures.

### 6.1. Deformations

The comparison of the maximum top-floor displacements calculated for the two passive PT frames (with low and high PT forces), and the two semi-active controllers (UDDA and FSFA) are shown in Figure 24-a. These results show that the use of semi-active control results in lower displacements than the low-passive (LPT) frames for all seismic inputs except Northridge (where they are similar). The deformations are generally slightly higher than those obtained with the high-passive frames, and the efficiency of the two semi-active controllers is similar, but varies from earthquake to earthquake. The 23% increase in top story displacement, recorded for UDDA control of the response to EL Centro input is due to the fact that reduction of top story displacement is not a control objective of the controller.

The maximum inter-story drift ratios (Figure 24-b), show that both UDDA and FSFA controllers result in smaller drifts than those in the passive frame with low PT forces, but larger than the drifts frames with high PT forces. The maximum UDDA drifts are close to those in frames with high PT forces but achieved at lower levels of base shear (except for Mexico City; Figure 25).

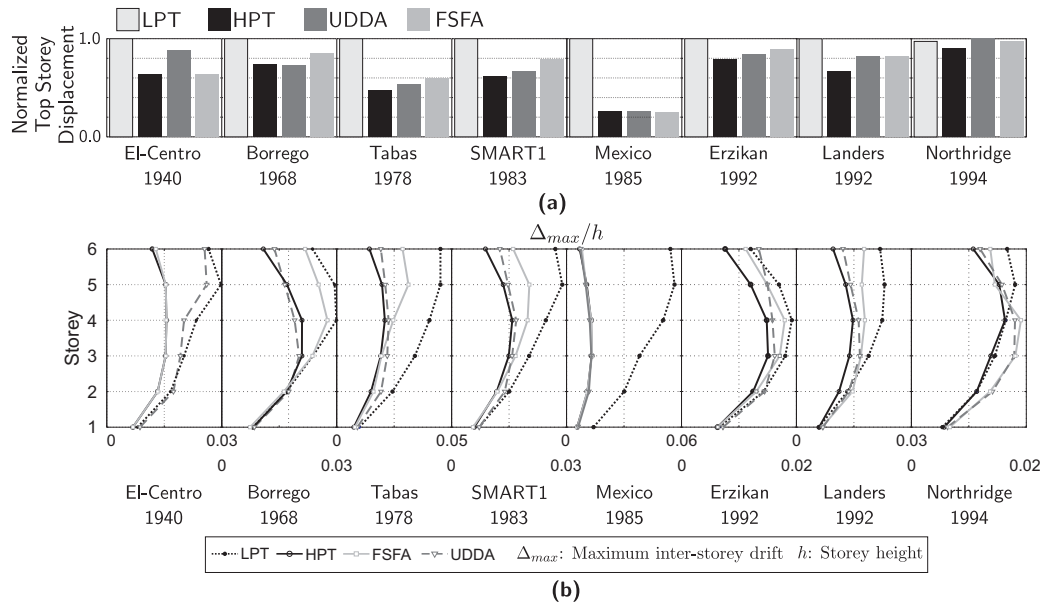


Figure 24. (a) Normalized maximum top story displacements for passive and semi-active controlled frames and (b) maximum inter-story drifts envelopes (LPT: Low PT force passive, HPT: High PT force passive, UDDA: semi-active, FSFA: semi-active).

## 6.2. Base shear and accelerations

A comparison of the maximum base shear recorded for the passive and semi-actively controlled structures is presented in Figure 25-a. It can be noticed that the two control algorithms (FSFA and UDDA) result in at least 10% (in some cases up to 20%) lower maximum base shear than that of the passive frame with high PT forces, and similar or up to 10% higher than the forces in the passive frame with low PT forces.

In both semi-active control approaches the changes in control forces were applied gradually, in order to take into account the practical limitations of rotating motors used for the control. This also resulted in avoiding sudden changes in the characteristics of the structure, which may lead to increased accelerations. The results of the simulations show that the maximum accelerations obtained with the semi-active systems were similar to those in the two passive frames (Figure 25-b).

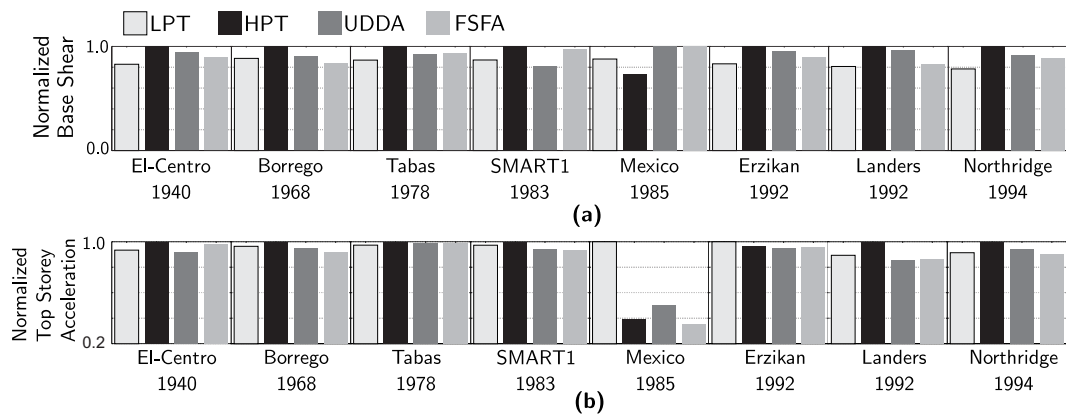


Figure 25. (a) Normalized maximum base shear and (b) Normalized maximum top story accelerations (LPT: Low PT force passive, HPT: High PT force passive, UDDA: semi-active, FSFA: semi-active).

## 7. CONCLUSIONS

In this paper are presented two centralized approaches for controlling the seismic response of post-tensioned steel frames by using a novel active control of post-tensioning forces of the strands. Two control approaches were investigated: (i) stiffness control approach and (ii) deformation regulation control approach.

The stiffness control approach has been proposed in previous research work and investigated for braced frames and truss structures. The key part of algorithms based on control of the structural stiffness is the selection algorithm. In this paper a novel stiffness selection algorithm (FSFA) is proposed based on Fourier analysis of the earthquake input (acceleration at the base) during the seismic action.

The second control approach is based on regulating the deformation of PT frames along the height of the structure. This is a new approach, which has never been investigated before. The main objective is not to reduce the inter-story drifts of all floors simultaneously, but to create a uniform distribution of inter-story drifts and reduce the maximum frame deformations. This regulation is achieved by changing the resistance of the PT connections, increasing in some stories and reducing in other storeys, based on the differences in inter-story drift along the height of the building (Uniform Drift Distribution Algorithm - UDDA). The result is a better distribution of internal forces in the elements throughout the structure.

The results obtained in simulations using the two new control systems show that compared to passive frames with high PT forces, the semi-active controllers reduce the forces in the structural elements, but increase the deformations. Compared to passive frames with low PT forces, the semi active control reduces the deformations with a small increase in base shear. In other words the response of the actively controlled frames is between the two limit cases of passive PT frames, regardless of the type of seismic input. This study was carried out by using a small set of control parameters. The efficiency of the semi-active systems can be improved by further research focussed on optimization of the control algorithms.

## REFERENCES

1. Ricles J, Sause R, Garlock M, and Zhao C. (2001), "Posttensioned Seismic-Resistant Connections for Steel Frames". *Journal of Structural Engineering*, 127(2), 113-121.
2. Christopoulos C, Filiatrault A, Uang C, and Folz B. (2002a), "Posttensioned Energy Dissipating Connections for Moment-Resisting Steel Frames". *Journal of Structural Engineering*, 128(9), 1111-1120.
3. Bruneau M, Engelhardt M, Filiatrault M, Goel M, Itani M, Hajar J, Leon R, Ricles J, Stojadinovic B and Uang C. (2005), "Review of selected recent research on US seismic design and retrofit strategies for steel structures". *Earthquake Engineering and Structural Dynamics*, 7, 103-114.
4. Garlock M, Sause R, and Ricles J. (2007), "Behaviour and Design of Posttensioned Steel Frame Systems". *Journal of Structural Engineering*, 133(3), 389-399.
5. Rojas P, Ricles J, and Sause R. (2005), "Seismic Performance of Post-tensioned Steel Moment Resisting Frames with Friction Devices". *Journal of Structural Engineering*, 131(4), 529-540.
6. Christopoulos C, Filiatrault A, and Folz B. (2002b), "Seismic Response of Self-centring Hysteretic SDOF Systems". *Earthquake Engineering and Structural Dynamics*, 31(5), 1131-1150.
7. Wang D. (2004), "Seismic Response of Steel Framed Hospital Buildings with Self-Centering Systems", MCCER Buffalo publication, in Student Research Accomplishments Volume: 2004-2005. Available at: <http://mceer.buffalo.edu/publications/resaccom/06-sp04/pdf/03wang.pdf>
8. Dimopoulos A, Karavasilis T, Vasdravellis G, and Uy B. (2013), "Seismic design, modelling and assessment of self-centering steel frames using post-tensioned connections with web hourglass shape pins". *Bulletin of Earthquake Engineering*, in press.
9. Horvat D, Barak P and Rabins M. (1983), "Semi-active Versus Passive or Active Tuned Mass Dampers for Structural Control". *Journal of Engineering Mechanics*, 109(3), 691-705.
10. Dyke S J, Spencer Jr. B F, Sain M K, and Charlson J D. (1996), "Seismic Response Reduction Using Multiple Magneto-rheological Dampers". *Proceedings of the IFAC world Congress*, San Francisco CA, June 30 July 5.
11. Markis N and McMahon S. (1996), "Structural control with controllable fluid dampers: design and implementation issues". *Proceedings of Second International Workshop on Structural Control*, Hong Kong, 311-322.
12. Ribakov, Y. (2003), "Predictive controlled stiffness devices in MDOF structures", *Journal of Structural Control*, 10(2), 101-115.
13. Ribakov, Y. (2004), "Semi-active predictive control of non-linear structures with controlled stiffness devices and friction dampers", *Structural Design of Tall and Special Buildings*, 3(2) 165-178.
14. Kobori T, Takahashi M, Nasu T, Niwa N and Ogasawara K. (1993), "Seismic response controlled structure with active variable stiffness system". *Earthquake Engineering and Structural Dynamics*, 22(11), 925-941.

15. Nemir D, Lin Y and Osegueda R. (1994), "Semi-active Motion Control Using Variable Stiffness". *Journal of Structural Engineering*, 120(4), 1291- 1306.
16. Lane J.S, Ferri A.A, and Heck B.S. (1992), "Vibration Control Using Semi-Active Friction Damping. Friction-Induced Vibration", *Chatter, Squeal, and Chaos*, American Society of Mechanical Engineers, Design Engineering Division (49), 165-171.
17. Inaudi J.A. (1997), "Modulated Homogenous Friction: A Semi-Active Damping Strategy". *Earthquake Engineering and Structural Dynamics*, 26(3), 361376.
18. Nishitani A, Nitta Y, and Ikeda Y. (2003), "Semi-active Structural Control Based on Variable Slip-Force Level Dampers". *Journal of Structural Engineering*, 129(7), 933-940.
19. Iskhakov I, and Ribakov Y. (2008), "Seismic Response of Semi-Active Friction-Damped Reinforced Concrete Structures with Self-Variation Stiffness". *The Structural Design of Tall and Special Buildings*, 17, 351-365.
20. Duerr K, Tesfamariam S, Wickramasinghe V, and Grewal A. (2013), "Variable Stiffness Smart Structure System to mitigate Seismic Induced Building Damages". *Earthquake Engineering and Structural Dynamics*, 42, 221-237.
21. Eljajeh Y and Petkovski M. (2013), "Control of strands forces for improving the seismic behaviour of post-tensioned steel frames". *Proceedings of the International Conference on Earthquake Engineering*, 29 to 31 May 2013- Skopje.
22. Nasu T, Kobori T, Motoichi T, Niwa N and Ogasawara K. (2001), "Active variable stiffness system with non-resonant control". *Earthquake Engineering and Structural Dynamics*, 30(11), 1597-1614.
23. Hajirasouliha I, Asadi P, Pilakoutas K.(2012), "An efficient performance-based seismic design method for reinforced concrete frames", *Earthquake Engineering and Structural Dynamics*, 41(4), 663-679.
24. Eurocode 8. (2004), "Design of structures for earthquake resistance- Part 1: General rules, seismic actions and rules for buildings". BS EN 1998-1:2004.
25. Federal Emergency Management Agency (FEMA). (2006), "Next-Generation Performance-Based Seismic Design Guidelines; Program Plan for New and Existing Buildings". FEMA, Rep. No. 445, Washington, D.C.
26. Eurocode 3. (2001), "Design of steel structures Part 1.1: General rules and rules for buildings". DD ENV 1993-1-1:1992.
27. Eljajeh Y and Petkovski M. (2013). "Connection Element for Modelling of Post-tensioned Steel Frames". *Second Conference on Smart Monitoring, Assessment and Rehabilitation of Civil Structures*. Istanbul, Turkey, 9-11 September, 2013.
28. Dobosy M, Garlock M, and VanMarcke M. (2006). "Comparison of Two Self-Centering Steel Moment Frame Modelling Techniques: Explicit Gap Models and Non-Linear Rotational Spring Models". *4<sup>th</sup> International Conference on Earthquake Engineering*, Taipei, Taiwan, October 12-13, 2006. Paper No.101.
29. Eljajeh Y. (2013). "Semi-Active Control of Post-tensioned Steel Frames". PhD thesis. The University of Sheffield. Sheffield. UK.
30. Regents of the University of California. (2000), "PEER Strong Motion Database". Available at: <http://peer.berkeley.edu/smcat/search.html>
31. Carr A J. (2007) "Ruaumoko Manual- Volume 1, Theory". University of Canterbury, New Zealand, available at: <http://www.ruaumoko.co.nz/manuals/RuaumokoTheory.pdf>
32. Somerville P, Smith N, Punyamurthula S, Sun J.Woodward-Clyde. (1997), federal services. "Development of Ground Motion Time Histories for Phase 2 of the FEMA/SAC Steel Project". SAC/BD-97/04 SAC joint venture, Sacramento, CA. 1997.
33. ASCE 41-13. (2013), "ASCE 41-13: Seismic Evaluation and Upgrade of Existing Buildings". American Society of Civil Engineers. Reston, Virginia.
34. Leitmann G. (1994), "Semi-active Control for Vibration Attenuation". *Journal of Intelligent Material Systems and Structures*, 5(6), 841 - 846.
35. Sadek F, and Mohraz B. (1998), "Semiactive Control Algorithms for Structures with Variable Dampers". *Journal of Engineering Mechanics*, 124(9), 981-990.
36. Dyke S, Spencer Jr. B, Sain M, and Charlson J. (1996), "Modeling and Control of Magnetorheological Dampers for Seismic Response Reduction". *Smart Materials and Structures*. 5, 565 -575.
37. Dyke S and Spencer Jr. B. (1997), "A Comparison of Semi-Active Control Strategies for the MR Damper". *Proceedings of the IASTED International Conference. Intelligent Information Systems*. The Bahamas, Dec 8-10, 1997.
38. Zhou L, Chang C, Wang L. (2003), "Adaptive Fuzzy Control for Nonlinear Building Magnetorheological Damper System". *Journal of Structural Engineering*, 129(7), 905-913.
39. Bitaraf M, Ozbulut O, Hurlbaas S, Barroso L. (2010), "Application of Semi-Active Control Strategies for Seismic Protection of Buildings with MR Dampers". *Engineering Structures*, 32, 3040-3047.
40. Bhardwaj M, and Datta T. (2006), Semiactive Fuzzy Control of the Seismic Response of Building Frames. *Journal of Structural Engineering*, 132(5), 791-799.